



*The Abdus Salam*  
**International Centre for Theoretical Physics**

  
United Nations  
Educational, Scientific  
and Cultural Organization

  
International Atomic  
Energy Agency

**H4.SMR/1775-31**

**"8th Workshop on Three-Dimensional Modelling of  
Seismic Waves Generation, Propagation and their Inversion"**

**25 September - 7 October 2006**

**Lehmann discontinuity beneath North America:  
No role for seismic anisotropy**

*Lev Vinnik*

**Institute of Physics of the Earth  
Moscow, Russia**

# Lehmann discontinuity beneath North America: No role for seismic anisotropy

L. Vinnik

Institute of physics of the Earth, Moscow, Russia

E. Kurnik

Faculty of Physics, Moscow State University, Moscow, Russia

V. Farra

Department de Sismologie, Institute du Physique du Globe de Paris, Paris, France

Received 29 December 2004; revised 25 February 2005; accepted 21 April 2005; published 13 May 2005.

[1] The Lehmann discontinuity in the upper mantle is often interpreted as a boundary separating anisotropic and isotropic media. We demonstrate, however, that seismic anisotropy plays, if any, a minor role in the origin of the Lehmann discontinuity. Our data are obtained with S receiver function technique from recordings of the MOMA seismograph array in the eastern USA. Part of the data is processed with a new modification of this technique. We observe Sp phase converted from the Lehmann discontinuity at a depth around 200 km with comparable amplitudes and similar polarities in two azimuths differing by about  $90^\circ$ . Contrary to the observations, the polarity in the synthetic seismograms for models with azimuthal anisotropy is opposite for the azimuths differing by  $90^\circ$ . Radial anisotropy with a slow vertical direction results in the Sp phase with the polarity opposite to the observed one. **Citation:** Vinnik, L., E. Kurnik, and V. Farra (2005), Lehmann discontinuity beneath North America: No role for seismic anisotropy, *Geophys. Res. Lett.*, 32, L09306, doi:10.1029/2004GL022333.

## 1. Introduction

[2] The seismic boundary at a depth between about 200 km and 250 km is often termed the Lehmann (or L) discontinuity. *Lehmann* [1961] interpreted it as the base of the low S velocity layer. *Leven et al.* [1981] argued that the L discontinuity is an effect of azimuthal anisotropy. *Dziewonski and Anderson* [1981] incorporated radial anisotropy into the PREM model. *Karato* [1992] suggested that the L discontinuity presents a rheological boundary between dislocation creep in the upper medium and diffusion creep in the lower one. Lattice preferred orientation of olivine which is responsible for seismic anisotropy in the upper mantle can only be induced by dislocation creep. Hence this model implies that the discontinuity separates anisotropic and isotropic media. The idea of a rheological boundary is supported in several studies [e.g., *Gaherty and Jordan*, 1995; *Gung et al.*, 2003; *Deuss and Woodhouse*, 2004], but the work of *Leven et al.* [1981] which initiated the chain of papers on the L discontinuity as a rheological boundary has never been verified by a demonstration of the

corresponding azimuthal variations in the properties of this discontinuity.

[3] In this study we address the problem of nature of the L discontinuity with a novel seismological approach: S receiver function technique [*Farra and Vinnik*, 2000]. This method is applied to the recordings of the MOMA array (Figure 1). P receiver functions for this array were obtained earlier, and observations of Ps converted phases from a discontinuity at a depth around 270–280 km were reported by *Li et al.* [2002].

## 2. Method

[4] S receiver function is the response of the Earth in the vicinity of a seismograph station to excitation by either SV or SH components of a teleseismic S wave. To detect the Sp phases, the 3-component seismogram is decomposed into P, SV, T and M components [*Farra and Vinnik*, 2000]. The SV axis corresponds to the principal S particle motion direction in the wave propagation plane. The P axis is perpendicular to SV in the same plane and is optimal for detecting Sp phases. The T axis is perpendicular to SV and P. The M axis corresponds to the principal motion direction of the S wave in the T-SV plane and is characterized by the angle  $\theta$  with the SV axis. The P components are deconvolved by their respective M components. Combined processing of the deconvolved P components of many seismic events yields  $P_c$  and  $P_s$ , the response of the Earth's medium to SV and SH components of S, respectively.

[5] The solution for either  $P_c$  or  $P_s$  is equivalent to stacking of the deconvolved P components of many recordings with weights depending on their respective  $\theta$  and variance of noise. The procedure of record processing involves evaluation of the rms value of the random noise in the stack. To account for the difference in slowness between the Sp phases and the parent phases, the estimates of  $P_c$  and  $P_s$  are obtained by stacking the deconvolved P components with moveout time corrections. The corrections are obtained as a product of differential slowness (the difference in slowness between the signal and the parent phase) and differential distance (the difference between the epicentral distance of the event and the average epicentral distance). In this paper we consider only  $P_c(t)$ , the P component deconvolved by the SV component of the

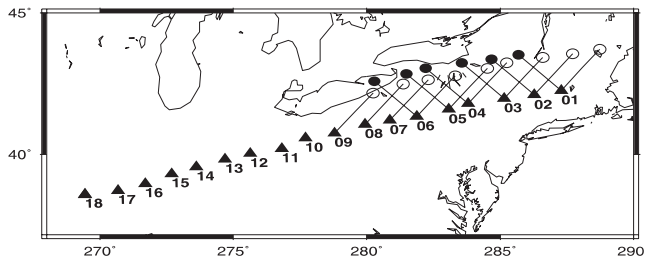


**Figure 1.** Map of the region with seismograph stations (triangles). Average positions of the piercing points of rays of the Sp phases at the Lehmann discontinuity are shown by filled (events from NW) and open (events from NE) circles.

parent phase. The analysis of  $P_s(t)$  is more complicated, and it cannot be presented in this short paper.

[6] The main problem of modeling the S receiver functions stems from the fact that the S wave train in the distance interval of interest consists of the S phase with the slowness around  $11.0 \text{ s}^\circ$  and SKS and ScS with the slowness around  $6.0 \text{ s}^\circ$ . In the modeling satisfactory results can be obtained with reflectivity synthetics by assuming that the converted phases are generated by the S wave at epicentral distances less than  $90^\circ$  and by SKS phase at larger distances [Vinnik *et al.*, 2004]. Another way to deal with the S/SKS interference problem is to separate the wave fields generated by the S and SKS by using a receiver array and to calculate the receiver functions and stack them separately for the S and SKS. This approach is proposed and first time tested in the present study.

### 3. Data and Results

[7] The Missouri to Massachusetts Broadband Seismometer Experiment (MOMA) array is around 2000 km long (Figure 1). From the east to the west it crosses the Palaeozoic Appalachian orogen and the Precambrian craton of North America. The Appalachian front bounding the Palaeozoic province in the west is located between station 7 and 8. S receiver function analysis requires seismic events in a distance range from around  $65^\circ$  to  $105^\circ$ . During about 18 months of operation the array recorded a number of seismic events in this distance range. The events are clustered in the back azimuth intervals between  $300^\circ$  and  $360^\circ$  (the north-western Pacific, 34 events), between  $10^\circ$  and  $60^\circ$  (Eurasia, 10 events) and between  $140^\circ$  and  $210^\circ$  (South America and southern Atlantic, 21 events). The recordings of these three groups were processed separately. To attain the highest signal/noise ratio the raw recordings were low-pass filtered with a corner at around 8 s. The number of seismic events in every group was too small for obtaining a sufficiently high signal/noise ratio at a single station, and individual receiver functions of several neighbouring stations were stacked as if they belonged to the same station.

[8] A relatively large number of events of the first group permits us to obtain useful results by stacking the receiver functions of only three neighbouring stations. In the stack for stations 1–3 (Figure 2a) we observe a clear Sp phase with negative polarity from the Moho at a time near  $-5 \text{ s}$

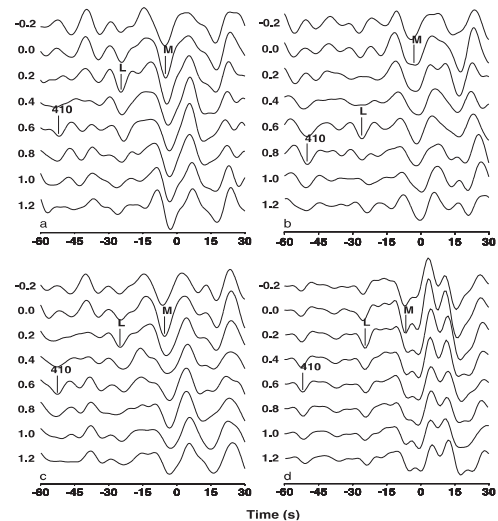


**Figure 2.** Stacked receiver functions for NW seismic events. Numbers on the left present the differential slowness in  $\text{s}^\circ$ . The detected phases are marked on the traces with the largest amplitudes. Labels M, L and 410 are for the Sp phases from the Moho, Lehmann and “410-km” discontinuities. The average (reference) epicentral distance is  $86^\circ$ . (a) Stack of 72 receiver functions of stations 1–3, rms value of noise is 0.01; (b) stack of 96 receiver functions of stations 7–9, rms value of noise is 0.007; (c) stack of 135 receiver functions of stations 1–6, rms value of noise is 0.007; (d) synthetic stack for stations 1–6 for the S velocity model MOMA in Figure 3.

and a phase with the same polarity at a time of  $-25 \text{ s}$  and the differential slowness of  $0.2 \text{ s}^\circ$ . Amplitude of this phase normalized to the amplitude of SV is around 0.05, very high relative to the rms value of noise (0.01). The negative polarity means that this phase is converted from a positive boundary (S velocity is higher at the lower side of the boundary). The depth of this discontinuity is around 200 km, and it can be interpreted as the L discontinuity. The phase with positive polarity at a time around  $-40 \text{ s}$  might be converted from the top of a very deep low S velocity layer [Vinnik and Farra, 2002]. The Sp phase from the “410 km” discontinuity is recorded at the time around  $-52 \text{ s}$ , but the signal is weak.

[9] A broadly similar wave field with the signals from the Moho, L and “410 km” discontinuities is observed at

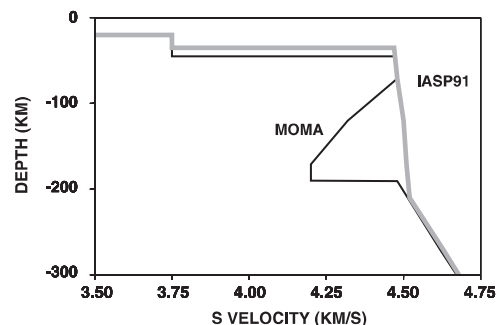


**Figure 3.** Preferred (MOMA) and standard (IASP91) isotropic S velocity models.

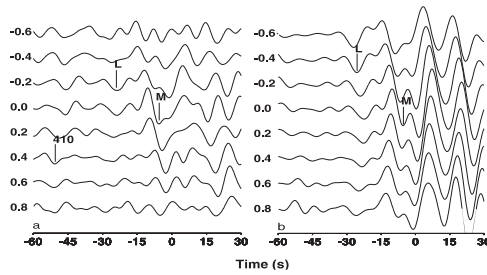


**Figure 4.** Stacked receiver functions of events from the NE: (a) stack of 57 receiver functions for stations 1–9, average epicentral distance is  $83^\circ$ , rms value of noise is 0.008; (b) stack of receiver functions of the events of Table 1 for the S phase. Amplitude scales are similar in this figure and Figure 2.

stations 7–9 (Figure 2b). The “410-km” signal arrives 2 s later than at stations 1–3. This indicates higher velocities at depths less than 410 km, which is consistent with other data [van der Lee and Nolet, 1997; van der Lee, 2002]. The signal from the L discontinuity arrives 1 s earlier. Taken together with the indications of a higher velocity this observation suggests a somewhat deeper (on the order of 10 km) L discontinuity. The number of useful recordings in the western half of the array is smaller than in the east, and in order to attain a sufficiently high signal/noise ratio for the western (Precambrian) region we stacked the receiver functions of 9 stations (10–18). No signals besides the Sp phases from the Moho and the “410 km” discontinuity were detected with confidence.

[10] The stack for stations 1–6 (Figure 2c) is representative for the eastern (Appalachian) region, and it demonstrates the same features as stations 1–3 in Figure 2a. The synthetic stack (Figure 2d) reproduces the times, amplitudes and polarities of the main seismic phases in the observed stack in Figure 2c. The related isotropic model (Figure 3) is obtained by modifying by trial and error IASP91 global model [Kennett and Engdahl, 1991]. The model differs from IASP91 by a thicker crust and by a low S velocity layer in the upper mantle. The bottom of the layer at a depth of 190 km represents the L discontinuity, in agreement with Lehmann [1961]. Considering the uncertainty of the adopted P and S velocities, the error of this depth estimate is on the order of  $\pm 5$  km. The related S velocity contrast of 0.3 km/s yields the amplitude of the Sp phase similar to the observed one in Figure 2c (0.037). The low velocity layer is required not only in order to reproduce the amplitude of the Sp phase from the Lehmann but also to obtain the right time of the signal from the “410 km” discontinuity. The assumption of a sharp L discontinuity in this model is arbitrary, and the sharpness of the upper boundary of the low velocity layer is not well constrained by the observations, as well.

[11] In the receiver functions of the southern events there is no clear evidence of a signal from the L discontinuity, but positive results are obtained for the events from the NE (Figure 4). The average back azimuth of the NE events ( $43^\circ$ ) differs by  $80^\circ$  from that of the NW events ( $323^\circ$ ). To attain a high signal/noise ratio in spite of a relatively small number of seismic events, we stacked the receiver functions

of 9 eastern stations. The surface projection of the piercing point of the Sp phase at the converting interface is displaced in the direction of the seismic event by a distance roughly similar to the depth of the discontinuity. Hence the receiver functions of 6 stations for the NW direction and of 9 stations for the NE direction sample roughly the same region of the L discontinuity (Figure 1). The stack of the NE receiver functions (Figure 4a) reveals a signal from the L discontinuity at about the same time as in Figure 2. The only significant difference is in the differential slowness ( $-0.2$  s/deg versus  $0.2$  s/deg).

[12] As we already mentioned, the receiver functions of the NW events provide evidence of the L discontinuity dipping to the SW and of the wave velocities rising in the same direction. These phenomena should change the differential slowness of the Sp phase from the L discontinuity for the NE events. In particular, ray tracing experiments demonstrate that a tilt of  $2^\circ$  and the lateral S velocity gradient in the upper mantle of  $0.0005$  km $^{-1}$  with a constant  $V_p/V_s$  ratio would reduce the differential slowness from  $0.2$  s/deg to  $-0.2$  s/deg. In other words, the observed change in differential slowness in Figure 4 is a predictable effect.

[13] For the NE events a difference in the epicentral distance at the edges of the group of 9 stations is sufficient for separating S and SKS phases by slant stacking the recordings of several stations. The slowness of the S in these experiments appears to be always lower than in global Earth models by about  $0.5$  s/deg. This is another indication of the wave velocity rising from NE to SW. Within this approach, first, we find the optimum slowness  $s_0$  of either S or SKS for a seismic event and perform slant stacking of the three components of recordings of this event for the slowness values of  $s_0 \pm k\delta s$ , where  $k = 0, 1, 2, \dots$  and  $\delta s = 0.2$  s/deg. Second, we transform the stacked three-component record for  $s_0$  into the receiver function exactly like we process an individual three-component record. Third, the stacked three-component recordings for  $k = 1, 2, \dots$  are transformed into the receiver functions by using the parameters of transformation that were obtained for  $s_0$ . Finally the receiver functions for different events are stacked for the differential slowness  $s_d = \pm k\delta s$ . The procedure can be termed double stacking, because it involves, first, stacking of recordings of the same event and, second, of the receiver functions of different events. The result for the four S phases (Table 1) thus obtained demonstrates (Figure 4b) the clear Sp phase with negative polarity at the time appropriate for the L discontinuity and at the differential slowness of  $-0.4$  s/deg. The amplitude of the signal from the L discontinuity in the stack for three SKS phases (not shown)

**Table 1.** Seismic Events Used for Double Stacking

Date d:m:y	Lat, deg	Lon, deg	Depth, km	Dist, deg	Baz, deg	$Slo_1^a$ , s/deg	$Slo_2^b$ , s/deg
23:02:95	35.0	32.3	150	76.9	51.8	9.5	
13:05:95	40.1	21.7	13	70.2	53.6	11.0	
16:05:95	36.5	70.9	190	96.8	25.6		5.0
15:06:95	38.4	22.3	140	72.2	54.3	11.0	7.2
01:10:95	38.1	30.2	33	73.6	51.1	10.0	
22:11:95	28.8	34.9	10	85.7	54.8		6.5

<sup>a</sup>Slowness of S.

<sup>b</sup>Slowness of SKS/ScS.

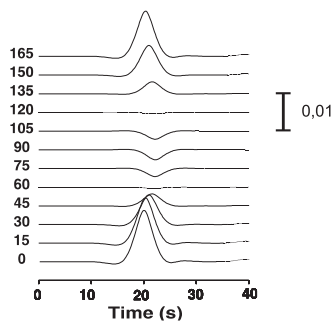


**Figure 5.** P components of synthetic seismograms of the Sp phase from the boundary between anisotropic and isotropic media. Numbers on the left are back azimuths in degrees.

appeared to be anomalously large. It can be an effect of noise.

#### 4. Discussion and Conclusions

[14] We have detected the Sp converted phase from the L discontinuity at a depth around 200 km with about the same time and amplitude in the back azimuths differing by nearly 90 degrees. The discontinuity is at the base of a well pronounced low S velocity layer in the east of the MOMA array. The low velocity layer was previously found near the eastern end of the array [van der Lee and Nolet, 1997; van der Lee, 2002], but our data require that it extends farther to the SW. The change of depth of the L discontinuity correlated with the change of the velocities along the array is consistent with the global trend reported by Deuss and Woodhouse [2004]. The failure to detect a similar signal in the P receiver functions of the same stations [Li et al., 2002] is a predictable effect of limitations of the P receiver function techniques: the Ps phase from a depth of 190 km arrives in the time interval dominated by crustal reverberations. We don't observe a signal from the discontinuity at a depth of 270–280 km, reported by Li et al. [2002].

[15] Seismic data reveal in the Earth's mantle two kinds of anisotropy. A discrepancy in the SV and SH velocities in the surface waves is interpreted in terms of radial anisotropy (anisotropy with a vertical symmetry axis). Shear wave splitting in the SKS phase is indicative of azimuthal anisotropy (anisotropy with a horizontal or tilted symmetry axis). The hypothesis of anisotropy can be tested with the aid of synthetic seismograms of the Sp phase from a boundary between anisotropic (top) and isotropic media (Figure 5). The theoretical seismograms are calculated with a code based on the Thomson-Haskell algorithm. Azimuthal anisotropy is modeled by hexagonal anisotropy with a horizontal axis of symmetry. Average velocities in the anisotropic layer are equal to isotropic velocities beneath the discontinuity. Coefficients of anisotropy (the difference between the fast and slow velocities normalized to their average) are 0.05 and 0.03 for the P and S waves, respectively. The anisotropic layer is 190 km thick. Apparent velocity is 10 km/s. The wave pattern shown in Figure 5 rotates in the azimuth domain, depending on the azimuth of fast velocity. Negative polarity is observed around the slow direction. For the adopted fast direction of 0°, negative

polarity of the Sp phase is observed in the back azimuths between 60° and 120°. Contrary to the observations, the synthetic Sp phase changes polarity when the azimuth changes by 90°. This property is very general, and it is preserved if the symmetry axis is tilted by several tens of degrees.

[16] Numerical experiments with a radial anisotropy were conducted for the parameters qualitatively similar to those in PREM (slow vertical direction). For the coefficients of the P and S wave anisotropy of 0.05 and 0.03 and apparent velocities of 8–12 km/s, normalized amplitudes of the Sp phase are between 0.01 and 0.02, of the same order as the observed ones, but the polarity is opposite. The right polarity can be obtained for anisotropy with a fast vertical axis. This assumption, however, contradicts seismic data [Beghein and Trampert, 2003].

[17] To conclude, a purely anisotropic nature of the L discontinuity is unlikely. The discontinuity presents the base of the low velocity layer. A change of anisotropy across this discontinuity still is possible, but as a minor effect, and another explanation for its properties is required.

[18] **Acknowledgments.** This study was supported by the Russian Fund for Basic Research, grant 04-05-64634. Recordings of the MOMA array were obtained from the IRIS DMC. The authors thank Karen Fischer for thoughtful review.

#### References

- Beghein, C., and J. Trampert (2003), Probability density functions for radial anisotropy: Implications for the upper 1200 km of the mantle, *Earth Planet. Sci. Lett.*, *217*, 151–162.
- Deuss, A., and J. H. Woodhouse (2004), The nature of the Lehmann discontinuity from its seismological Clapeyron slopes, *Earth Planet. Sci. Lett.*, *225*, 295–304.
- Dziewonski, A. M., and D. L. Anderson (1981), Preliminary Reference Earth Model (PREM), *Phys. Earth Planet. Inter.*, *25*, 297–356.
- Farra, V., and L. P. Vinnik (2000), Upper mantle stratification by P and S receiver functions, *Geophys. J. Int.*, *141*, 699–712.
- Gaherty, J. B., and T. H. Jordan (1995), Lehmann discontinuity as the base of an anisotropic layer beneath continents, *Science*, *268*, 1468–1471.
- Gung, Y., M. Panning, and B. Romanowicz (2003), Global anisotropy and the thickness of continents, *Nature*, *422*, 707–710.
- Karato, S. (1992), On the Lehmann discontinuity, *Geophys. Res. Lett.*, *19*, 2255–2258.
- Kennett, B. L. N., and E. R. Engdahl (1991), Traveltimes for global earthquake location and phase identification, *Geophys. J. Int.*, *105*, 429–465.
- Lehmann, I. (1961), S and the structure of the upper mantle, *Geophys. J. R. Astron. Soc.*, *4*, 124–138.
- Leven, J. H., I. Jackson, and A. E. Ringwood (1981), Upper mantle seismic anisotropy and lithospheric decoupling, *Nature*, *289*, 234–239.
- Li, A., K. M. Fischer, S. van der Lee, and M. E. Wysession (2002), Crust and upper mantle discontinuity structure beneath eastern North America, *J. Geophys. Res.*, *107*(B5), 2100, doi:10.1029/2001JB000190.
- van der Lee, S. (2002), High-resolution estimates of lithospheric thickness from Missouri to Massachusetts, USA, *Earth Planet. Sci. Lett.*, *203*, 15–23.
- van der Lee, S., and G. Nolet (1997), Upper mantle S velocity structure of North America, *J. Geophys. Res.*, *102*, 22,815–22,838.
- Vinnik, L., and V. Farra (2002), Subcratonic low-velocity layer and flood basalts, *Geophys. Res. Lett.*, *29*(4), 1049, doi:10.1029/2001GL014064.
- Vinnik, L. P., V. Farra, and R. Kind (2004), Deep structure of the Afro-Arabian hotspot by S receiver functions, *Geophys. Res. Lett.*, *31*, L11608, doi:10.1029/2004GL019574.

V. Farra, Department de Sismologie, CNRS UMR 7580, Institut du Physique du Globe de Paris, 4 Place Jussieu, F-75252 Paris cedex, France. (farra@ipgp.jussieu.fr)

E. Kurnik, Faculty of physics, Moscow state University, Leninskiye Gori, 119992 Moscow, Russia.

L. Vinnik, Institute of physics of the Earth, 123995 Moscow, B. Grouzinskaya 10, Russia. (vinnik@ifz.ru)